

Statefinder parameters for quantum effective Yang-Mills condensate dark energy model

Minglei Tong*, Yang Zhang and Tianyang Xia
Astrophysics Center
University of Science and Technology of China
Hefei, Anhui, China

Abstract

The quantum effective Yang-Mills condensate (YMC) dark energy model has some distinguished features that it naturally solves the coincidence problem and, at the same time, is able to give an equation of state w crossing -1 . In this work we further employ the Statefinder pair (r, s) introduced by Sahni et al to diagnose the YMC model for three cases: the non-coupling, the YMC decaying into matter only, and the YMC decaying into both matter and radiation. The trajectories (r, s) and (r, q) , and the evolutions $r(z)$, $s(z)$ are explicitly presented. It is found that, the YMC model in all three cases has $r \simeq 1$ for $z < 10$ and $s \simeq 0$ for $z < 5$ with only small deviations $\simeq 0.02$, quite close to the cosmological constant model (LCDM), but is obviously differentiated from other dark energy models, such as quiescence, kinessence etc.

keywords: Yang-Mills condensate, dark energy, Statefinder

PACS numbers: 98.80.-k, 98.80.Es, 95.36.+x, 04.62.+v

*mltong@mail.ustc.edu.cn

1 Introduction

The currently accelerating expansion of the universe has been indicated by the observation of Type Ia supernovae [1], and is consistent with the data from cosmic microwave background (CMB) [2, 3] and from the cosmic large scale structure [4]. The acceleration of the expanding universe is attributed to the dominant dark energy $\Omega_\Lambda \simeq 0.73$, coexisting with the matter $\Omega_m \simeq 0.27$. The simplest model for dark energy is the cosmological constant [5], with an equation of state (EOS) $w = -1$ as the universe evolves. However, two questions arise from this scenarios, namely, the fine-tuning problem and the cosmic coincidence problem. While the former exists for almost all the dark energy models, the latter has been addressed in the class of dynamical dark energy models, which take some dynamically-evolving field as the candidate for the dark energy. Among them are the quintessence [6], phantom [7], k-essence [8], quintom [9], tachyonic [10], holographic dark energy model [11], and interacting dark energy model [12]. Besides, there is another interesting type of model built on the quantum effective gravity [13], which includes the quantum corrections of gravitational field to Einstein equations. Different from these models, the Yang-Mills condensate dark energy model is based on a vector-type of the quantum effective Yang-Mills field [14, 15, 16, 17, 18]. From field-theoretical point of view, the model has the following interesting properties: the gauge fields are indispensable to the Standard Model of particle physics, and the effective Lagrangian of YMC is determined from the standard field-theoretical calculations for each order of loops of quantum corrections, and thereby gives the correct trace-anomaly, and there is room for change its form by hand. Moreover, it is found that, for quite generic initial conditions, the YMC dark energy model always has the desired tracking behavior that naturally solves the coincidence problem. This has been accomplished for the cases of 1-loop [16, 17], 2-loop [18], and 3-loop [19] quantum corrections, either with coupling or without coupling to matter and/or radiation. When coupling with matter, or with both matter and radiation, the YMC has an EOS crossing -1 smoothly and taking $w \sim -1.05$, as indicated by the recent preliminary observational data of the Supernova Legacy Survey [20, 21].

In order to differentiate these various dark energy models, Sahni et al [22] introduce a new geometrical diagnostic pair (r, s) , called Statefinder, which involves the third order time-derivative of scale factor. The pair is related to the EOS of dark energy and its time derivative. From the observational side, the values of (r, s) can be extracted from data coming from SNAP type experiments [23]. The Statefinder diagnosis has been applied to several dark energy models [24, 25, 26, 27]. In particular, the spatially flat LCDM has a fixed point $(r, s) = (1, 0)$. For the 1-loop YMC dark energy model, Ref.[28] studies the non-coupling case with the radiation contribution being neglected. In this paper for a complete treatment of the Statefinder diagnosis, we work with the 2-loop coupling YMC model and include the radiation component. Thereby, there arise considerable modifications to the 1-loop non-coupling case.

2 2-loop YMC dark energy model

We consider a spatially flat($k = 0$) Robertson-Walker (RW) universe, whose expansion is determined by the Friedmann equations

$$H^2 = \frac{8\pi G}{3}\rho, \quad (1)$$

$$\frac{\ddot{a}}{a} = -\frac{4\pi G}{3}(\rho + 3p), \quad (2)$$

where $H = \frac{\dot{a}}{a}$, the pressure $p(t) = p_y + p_r$, the energy density $\rho(t) = \rho_y + \rho_m + \rho_r$, with the subscripts ‘ y ’, ‘ m ’ and ‘ r ’ refer to the YMC dark energy, the matter (including both baryons and dark matter), and the radiation, respectively. Up to the 2-loop quantum corrections, the energy density ρ_y and the pressure p_y of the YMC are given by [18, 19]

$$\rho_y = \frac{b}{2}F \left[y + 1 + \eta \left(\ln |y - 1 + \delta| + \frac{2}{y - 1 + \delta} \right) \right], \quad (3)$$

$$p_y = \frac{b}{6}F \left[y - 3 + \eta \left(\ln |y - 1 + \delta| - \frac{2}{y - 1 + \delta} \right) \right], \quad (4)$$

where $y \equiv \ln |F/\kappa^2|$, $F \equiv E^2 - B^2$, κ is the renormalization scale with dimension of squared mass, $b = \frac{11N}{3(4\pi)^2}$ for the gauge group $SU(N)$ without fermions, $\eta \equiv \frac{2b_1}{b^2} \simeq 0.84$ with $b_1 = \frac{17N^2}{3(4\pi)^4}$ representing the 2-loop contribution, and the dimensionless constant δ is a parameter representing higher order corrections. For simplicity, we take the gauge group to be $SU(2)$ and only consider the ‘electric’ condensate, i.e., $F = E^2$. The EOS for the YMC is

$$w = \frac{p_y}{\rho_y} = \frac{y - 3 + \eta \left(\ln |y - 1 + \delta| - \frac{2}{y - 1 + \delta} \right)}{3 \left[y + 1 + \eta \left(\ln |y - 1 + \delta| + \frac{2}{y - 1 + \delta} \right) \right]}. \quad (5)$$

When one sets $\eta = 0$ in the above expressions of Eqs.(3), (4), and (5), the 1-loop model is recovered [15, 16, 17]. At high energies $y \rightarrow \infty$, p_y is positive, and the EOS of YMC approaches to that of a radiation $w \rightarrow 1/3$, as is expected for an effective quantum field theory.

The dynamical evolutions of the three components of the universe are

$$\dot{\rho}_y + 3\frac{\dot{a}}{a}(\rho_y + p_y) = -\Gamma\rho_y - \Gamma'\rho_y, \quad (6)$$

$$\dot{\rho}_m + 3\frac{\dot{a}}{a}\rho_m = \Gamma\rho_y, \quad (7)$$

$$\dot{\rho}_r + 3\frac{\dot{a}}{a}(\rho_r + p_r) = \Gamma'\rho_y, \quad (8)$$

where Γ and Γ' are the decay rate of YMC into matter and radiation, respectively. Taking ρ_y in Eq.(3) to be the dark energy with $\rho_y(t_0) \sim 0.73\rho_c$, the scale κ is fixed by $\kappa^{1/2} \simeq 7.6h_0^{1/2} \times 10^{-3}$ eV, where $h_0 \sim 0.72$ is the current value of the Hubble parameter. For concreteness, $\delta = 3$ and $\eta = 0.84$ are taken.

The initial matter and radiation densities at $z \simeq 3454$ [3] are taken to be $x_i = R_i \simeq 1 \times 10^{10}$, where $x \equiv \rho_m/\frac{1}{2}b\kappa^2$, and $R \equiv \rho_r/\frac{1}{2}b\kappa^2$. The initial YMC can be chosen to be in a broad range

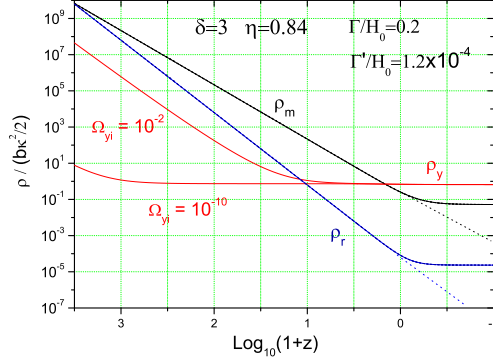


Figure 1: The evolution of the energy densities. In the non-coupling case $\rho_m \propto a(t)^{-3}$ and $\rho_r \propto a(t)^{-4}$ throughout. In the case of YMC decaying into matter, ρ_m deviates from $\propto a(t)^{-3}$ around $z \sim 0$ and levels off. In the case of YMC decaying into both matter and radiation, both $\rho_m(t)$ and $\rho_r(t)$ level off around $z \sim 0$. Note that two different initial condition: $\Omega_{yi} = 10^{-2}$ and 10^{-10} , yield the same ρ_y , ρ_m , and ρ_r at $z \sim 0$.

$y_i = (1, 15)$, corresponding to $\Omega_{yi} \simeq (10^{-10}, 10^{-2})$. For the case of YMC decaying into matter, we take $\Gamma/H_0 = 0.2$ with $H_0 = (\frac{4\pi G b \kappa^2}{3})^{1/2}$, approximately the Hubble constant. For the case of YMC decaying into both matter and radiation, we take $\Gamma/H_0 = 0.2$ and $\Gamma'/H_0 = 1.2 \times 10^{-4}$. Fig.1 shows the evolution of the energy densities for various components in all three cases. It is seen that, for the initial values of Ω_{yi} ranging eight orders of magnitude, the present status $\Omega_y \sim 0.73$, $\Omega_m \sim 0.27$, and $\Omega_r \sim 10^{-5}$, are achieved. In this sense, the coincidence problem of dark energy is naturally solved in the YMC model [15, 17, 18]. It is also found that in the coupling cases w can be cross -1 smoothly [18].

3 Statefinder

The Statefinder pair (r, s) are defined as the following [22]

$$r \equiv \frac{\ddot{a}}{aH^3}, \quad s \equiv \frac{r-1}{3(q-1/2)}, \quad (9)$$

where the deceleration parameter

$$q = -\frac{\ddot{a}}{aH^2} = \frac{1}{2}(1 + 3\Omega_y w + \Omega_r), \quad (10)$$

with $\Omega_y = \rho_y/\rho$ and $\Omega_r = \rho_r/\rho$. For completeness we include Ω_r , which is important in the early times. Taking time derivative of Eq.(2) and making use of Eqs.(6), (7), and (8) yield the following general form of the Statefinder pair

$$r = 1 + \frac{9}{2}\Omega_y w(1+w) - \frac{3}{2}\Omega_y \frac{\dot{w}}{H} + 2\Omega_r + \frac{3\Gamma}{2H}\Omega_y w + \frac{\Gamma'}{2H}\Omega_y(3w-1), \quad (11)$$

$$s = \frac{3\Omega_y w(1+w) - \Omega_y \frac{\dot{w}}{H} + \frac{4}{3}\Omega_r + \frac{\Gamma}{H}\Omega_y w + \frac{\Gamma'}{3H}\Omega_y(3w-1)}{3\Omega_y w + \Omega_r}, \quad (12)$$

which hold actually for a generic dark energy model.

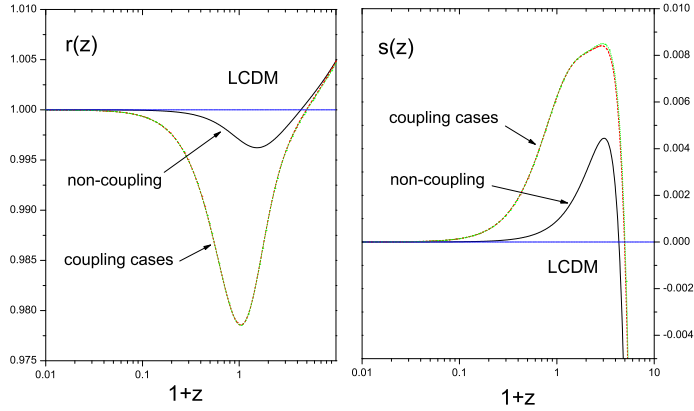


Figure 2: The left panel: $r(z) \simeq 1$ for $z < 10$ in the three cases of YMC. The right panel: $s(z) \simeq 0$ for $z < 5$. Thus $(r, s) \simeq (1, 0)$ with an error $\simeq 0.02$ in YMC, quite close to that of LCDM. The initial YMC fractional energy $\Omega_{yi} = 10^{-2}$ is taken.

Let us apply the pair to some simple models. For any LCDM with a non-zero cosmological constant Λ , one simply has $(r, s) = (1, 0)$, and $q(t) = (-1, \frac{1}{2})$. For the Steady State Universe (SSU) model [29] with $a(t) = e^{H_0 t}$ one also has $(r, s) = (1, 0)$, but it has a fixed $q(t) = -1$. For the standard cold dark matter model (SCDM), our calculation gives $(r, s) = (1, \frac{4}{3})$, which is different from the value $(r, s) = (1, 1)$ often quoted in literatures [22]. The details of our derivation is given in Appendix.

In the following we present (r, s) in the YMC model for three cases: the non-coupling, the YMC decaying into matter, the YMC decaying into both matter and radiation. The following plots are based on Eqs.(10), (11) and (12).

First, we discuss the evolutions of (r, s) . Fig.2 gives the behaviors of $r(z)$ and $s(z)$ in the recent past time with $z < 10$ in all the three cases of YMC model. It is clear that $r(z) \simeq 1$ for $z < 10$ and $s(z) \simeq 0$ for $z < 5$. Thus $(r, s) \simeq (1, 0)$ with an error $\simeq 0.02$ in YMC, quite close to that of LCDM. The two coupling cases, i.e., YMC decaying into matter, and into both matter and radiation, yield almost overlapping results since the YMC-radiation coupling $\Gamma'/H_0 \sim 10^{-4}$ is very small. Furthermore, we would like to analyze the behavior in the radiation stage. In the limit of large z , one has $\Omega_y \rightarrow \Omega_{yi} \simeq (10^{-10}, 10^{-2})$ and $\Omega_r \rightarrow 1 - \Omega_{yi} \simeq 1$, Eqs.(11) and (12) give an asymptotic behavior

$$r \rightarrow 3, \quad s \rightarrow \frac{4}{3}, \quad q \rightarrow 1, \quad (13)$$

independent of the initial condition. The analysis for the 1-loop YMC model in Ref.[17] did not include Ω_r , so the extrapolation to the radiation stage could not have been made.

To show the difference of YMC from other dark energy models, Fig.3 demonstrates $r(z)$ and $s(z)$ from YMC, LCDM, quiescence, and kinessence, respectively [22]. On the left panel, while YMC gives $r(z) = 1 \pm 0.02$ around $z \simeq 0$, quiescence and kinessence give their respective

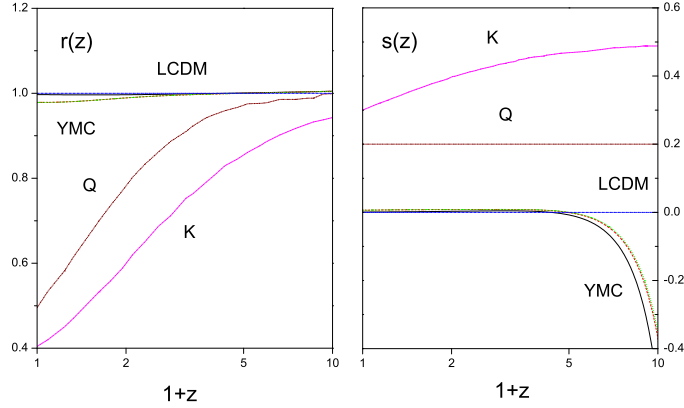


Figure 3: The details of $r(z)$ on the left and $s(z)$ on the right around $z = (0, 10)$ in YCM compared with quiescence (Q) and kinessence (K) models [22].

$r(z)$ decreasing to 0.5 and 0.4. On the right panel, for $z \leq 4$ in all three cases of YMC model, $s(z)$ approaches to 0, quite close to LCDM model. On the other hand, the quiescence has a constant $s = 0.2$, and the kinessence has $s(z) > 0.3$ around $z \simeq 0$. The differences of the YMC from quiescence and kinessence are very large. However, like the other dark energy models, $s(z)$ in YMC also has a divergence at $z \sim 13$, which does not show up in Fig.3.

In the following we discuss the $r - s$ plan and the $r - q$ plan in the three cases of YMC model.

Fig.4(a) gives the recent ($z < 0.8$) (r, s) trajectory in the non-coupling case of YMC. Two trajectories are presented for two initial values $y_i = 1$ and $y_i = 15$, respectively. The round dot at $(1.00016, 4.76 \times 10^{-5})$ is the current value for $y_i = 1$, and that at $(0.997, 9.07 \times 10^{-4})$ is for $y_i = 15$, respectively. The star at $(r, s) = (1, 0)$ is the fixed point of LCDM model, which currently is still robust against the observations. Our model predicts an asymptote at $t \rightarrow \infty$ very close to that of LCDM model. The trajectories of $y_i = 15$ and of $y_i = 1$ approach to it by different paths. With the expansion of the universe, all trajectories for different initial conditions will reach to the fixed point $(r, s) = (1, 0)$ ultimately. In comparison, the quiescence and kinessence models give the current values $r < 0.5$ and $s \sim 0.5$, other models have very scattered typical values, such as the quietessence model [24] with $(r, s) = (0.4, 0.3)$, the Chaplygin gas model [25] with $(r, s) = (1.95, -0.3)$, the agegraphic model [26] with $(r, s) = (-0.2, 0.5)$, which are far away from that of LCDM model [22]. The holographic model [27] without interaction has $(r, s) \simeq (0.94, 0.01)$, but an interaction $b^2 = 0.1$ gives $(r, s) \simeq (0.75, 0.09)$, deviating away from LCDM model again.

Fig.4(b) gives the recent ($z < 1.1$) (r, q) trajectory in the non-coupling case of YMC. For $y_i = 1$, r decreases to unity monotonically, whereas, for $y_i = 15$, r decreases to a minimum value then increases back to unity. The two trajectories eventually approach to the fixed point at $(1, -1)$ of the SSU. Note that, the pair (r, q) in YMC does not pass through the fixed point

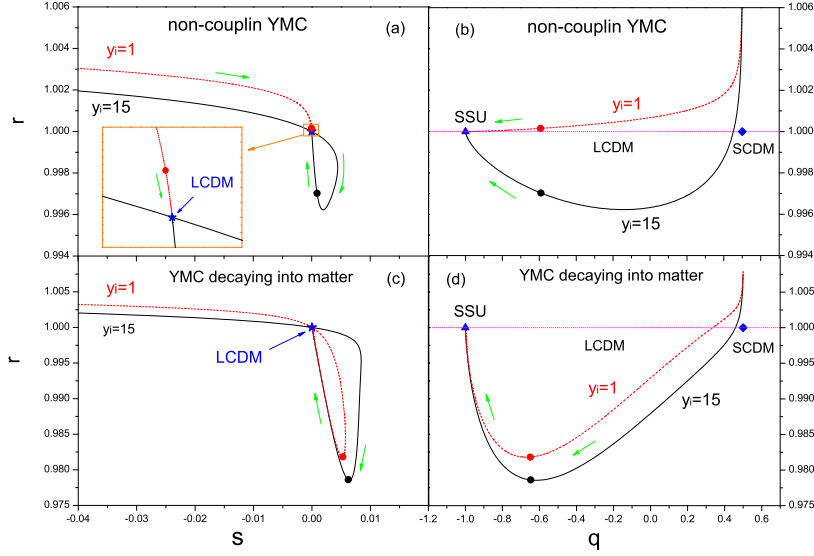


Figure 4: The recent trajectories (r, s) and (r, q) for the non-coupling case in (a) and (b) and for the YMC decaying into matter in (c) and (d). The round dots are the current values for the $y_i = 1$ and for $y_i = 15$, respectively. The arrows along the curves denote the evolution direction. The square dot at $(\frac{1}{2}, 1)$ is the fixed point of SCDM, and the triangle dot at $(-1, 1)$ is that of the Steady State Universe.

$(1, \frac{1}{2})$ of the SCDM [24].

Fig.4(c) shows the (r, s) trajectory in the case of YMC decaying into matter, whose overall profile looks similar to, but its detail is different from, that of the non-coupling case in Fig.4(a). The current values of the Statefinder pair $(r, s) = (0.981, 5.27 \times 10^{-3})$ for $y_i = 1$, and $(r, s) = (0.979, 6.21 \times 10^{-3})$ for $y_i = 15$, respectively. As $t \rightarrow \infty$, (r, s) will also approach the fixed point $(1, 0)$ of the LCDM model.

Fig.4(d) shows the (r, q) trajectory in the case of YMC decaying into matter, which is similar to that of non-coupling case in Fig.4(b), but the case for $y_i = 1$ has $r < 1$ due to the coupling. As $t \rightarrow \infty$, (r, q) will also approach the fixed point $(1, -1)$ of the SSU models. Moreover, in this case, the trajectories of (r, q) do not pass through the fixed point $(1, \frac{1}{2})$ of the SCDM either.

The case of YMC decaying into both matter and radiation. Their $r(z)$ and $s(z)$ are plotted in Fig.2. Since the YMC-radiation coupling Γ'/H_0 is very small, its modifications to the parameters r , s , and q are $\leq 10^{-3}$. Therefore, the trajectories (r, s) and (r, q) in this case are almost overlapped with Fig.4 (c) and (d), respectively. To save room, we do not plot the (r, s) and (r, q) in this case.

4 Summary

The Statefinder pair (r, s) is examined for the 2-loop quantum effective YMC dark energy model. Three cases are presented: the non-coupling YMC, the YMC decaying into matter,

and the YMC decaying into both matter and radiation. It is found that in all the three cases the pair (r, s) is very close to the fixed point $(1, 0)$ of LCDM model for $z < 5$, and the deviations are tiny $\delta r \sim 10^{-2}$ and $\delta s \sim 10^{-2}$. Among the three cases, (r, s) in the non-coupling case differs only by $\sim 1\%$ from those in the two coupling models, while the two coupling models are almost the same as each other in all aspects, since the decay rate of YMC into radiation is very small in the model. In regards to the diagnosis of Statefinder pair, the YMC model is shown to differ drastically from other dark energy models, such as quiescence, kinessence, quintessence, Chaplygin gas, interacting holographic, and agegraphic, etc. If further cosmological observations continue to support LCDM model, they are unlikely to rule out the YMC dark energy model by using only the pair (r, s) .

ACKNOWLEDGMENT: Y.Zhang's research work was supported by the CNSF No.10773009, SRFDP, and CAS.

Appendix

In this appendix we derive the Statefinder (r, s) for SCDM with $k = 0$, i.e., the Einstein-de Sitter model containing only matter. For the time being, however, we let the radiation density ρ_r be non-vanishing and will set $\rho_r = 0$ in the final step of calculation. The Friedman Equations are still given in Eqs.(1) and (2), while the total energy density $\rho = \rho_m + \rho_r$ and the total pressure $p = p_r$. There is no coupling between matter and radiation, so the energy is conserved for each component:

$$\begin{aligned}\dot{\rho}_m + 3H\rho_m &= 0; \\ \dot{\rho}_r + 3H(\rho_r + p_r) &= 0,\end{aligned}\tag{14}$$

which ensure that the total energy satisfies:

$$\dot{\rho} + 3H(\rho + p) = 0.\tag{15}$$

Taking time derivative of Eq.(2) leads to

$$\frac{\ddot{a}}{a} - \frac{\dot{a}\dot{a}}{a^2} = -\frac{4\pi G}{3}(\dot{\rho} + 3\dot{p}).\tag{16}$$

Then with the help of Eqs.(1), (2) and (15), one obtains,

$$r \equiv \frac{\ddot{a}}{aH^3} = 1 - \frac{3\dot{p}}{2H\rho}.\tag{17}$$

Applying Eq.(14) and taking $\dot{p} = \dot{p}_r = \frac{1}{3}\dot{\rho}_r$ into account, one obtains r for SCDM model,

$$r = 1 + 2\Omega_r.\tag{18}$$

By Eq. (2), the deceleration parameter q for SCDM model is given by

$$q = -\frac{\ddot{a}}{aH^2} = \frac{1}{2}(1 + \Omega_r). \quad (19)$$

Using the definition in Eq.(9), one has

$$s \equiv \frac{r - 1}{3(q - 1/2)} = \frac{2\Omega_r}{\frac{3}{2}\Omega_r} = \frac{4}{3}, \quad (20)$$

which is different from the value $s = 1$ that has been often quoted in literature [22]. Note that, since Ω_r is cancelled, this result of s is independent of the value of Ω_r . Setting $\Omega_r = 0$ in Eq.(18) yields the Statefinder pair of SCDM

$$(r, s) = \left(1, \frac{4}{3}\right). \quad (21)$$

References

- [1] A.G. Riess et al., *Astron. J.* **116** 1009 (1998);
A.G. Riess et al., *Astrophys. J.* **117** 707 (1999);
S. Perlmutter et al., *Astrophys. J.* **517** 565 (1999);
J.L. Tonry et al., *Astrophys. J.* **594** 1 (2003);
R.A. Knop et al., *Astrophys. J.* **598** 102 (2003);
A.G. Riess, et al., *Astron. J.* **607** 665 (2004).
- [2] P. de Bernardis et al., *Nature* **404** 955 (2000);
A.E. Lange et al., *Phys. Rev. D* **63** 042001 (2001);
A. Balbi et al., *Astroph. J.* **545** L1 (2001);
A. Benoit et al., *Astron. Astroph.* **399** L25 (2003).
- [3] C.L. Bennett, et al., *Astrophys. J. Suppl.* **148** 1 (2003);
D.N. Spergel, et al., *Astrophys. J. Suppl.* **148** 175 (2003);
H. V. Peiris et al., *Astrophys. J. Suppl.* **148** 213 (2003);
D.N. Spergel, et al., *Astrophys. J. Suppl. Ser.* **170** 377 (2007).
E. Komatsu, et al., arXiv:0803.0541.
G. Hinshaw, et al., arXiv:0803.0732.
J. Dunkley, et al., arXiv:0803.0586.
- [4] N.A. Bahcall, J.P. Ostriker, S. Perlmutter, P.J. Steinhardt, *Science* **284** 1481 (1999).
- [5] S. Weinberg, *Rev. Mod. Phys.* **61** 1 (1989);
S.M. Carroll, *Living Rev. Relativ.* **4** 1 (2001);
P.J.E. Peebles, B. Ratra, *Rev. Mod. Phys.* **75** 559 (2003);
T. Padmanabhan, *Phys. Rep.* **380** 235 (2003).
- [6] C. Wetterich, *Nucl. Phys. B* **302** 668 (1988); *Astron. Astrophys.* **301** 321 (1995);
B. Ratra, P.J.E. Peebles, *Phys. Rev. D* **37** 3406 (1988);
R.R. Caldwell, *Phys. Lett. B* **545** 23 (2002);
I. Zlatev, I. Wang, P.J. Steinhardt, *Phys. Rev. Lett.* **82** 896 (1999);
P.J. Steinhardt, L. Wang, I. Zlatev, *Phys. Rev. D* **59** 123504 (1999);

- [7] R.R. Caldwell, Phys. Lett. B **545** 23 (2002);
 S. M. Carroll, M. Hoffman, M. Trodden, Phys. Rev. D **68** 023509 (2003);
 R.R. Caldwell, M. Kamionkowski, N.N. Weinberg, Phys. Rev. Lett. **91** 071301 (2003);
 S. Nojiri, S.D. Odintsov, Phys. Lett. B **562** 147 (2003);
 M.P. Dabrowski, T. Stachowiak, M. Szydlowski, Phys. Rev. D **68** 103579 (2003).
- [8] C. Armendariz-Picon, T. Damour, V.F. Mukhanov, Phys. Lett. B **458** 209 (1999);
 C. Armendariz-Picon, V.F. Mukhanov, P.J. Steinhardt, Phys. Rev. Lett. **85** 4438 (2000);
 T. Chiba, T. Okabe, M. Yamaguchi, Phys. Rev. D **62** 023511 (2000);
 C. Armendariz-Picon, V.F. Mukhanov, P.J. Steinhardt, Phys. Rev. D **63** 103510 (2001);
 M. Malquarti, E.J. Copeland, A.R. Liddle, M. Trodden, Phys. Rev. D **67** 123503 (2003);
- [9] H. Wei, R.G. Cai, D.F. Zeng, Class. Quant. Grav. **22** 3189 (2005);
 W. Hu, Phys. Rev. D **71** 047301 (2005);
 B. Feng, X.L. Wang, X.M. Zhang, Phys. Lett. B **607** 35 (2005);
 Z.K. Guo, Y.S. Piao, X.M. Zhang, Y.Z. Zhang, Phys. Lett. B **608** 177 (2005);
 W. Zhao, Y. Zhang, Phys. Rev. D **73** 123509 (2006);
 R. Lazkoz, G. Leon, Phys. Lett. B **638** 303 (2006).
- [10] T. Padmanabhan, Phys. Rev. D **66** 021301 (2002);
 J.S. Bagla, H.K. Jassal, T. Padmanabhan, Phys. Rev. D **67** 063504 (2003);
 W. Fang, H.Q. Lu, Z.G. Huang, K.F. Zhang, Int. J. Mod. Phys. D **15** 199 (2006);
- [11] M. Li, Phys. Lett. B **603** 1 (2004);
 Q.G. Huang, Y. Gong, JCAP **0408** 006 (2004);
 Q.G. Huang, M. Li, JCAP **0408** 013 (2004); **0503** 001 (2005);
- [12] L. Amendola, Phys. Rev. D **62** 043511 (2000);
 Z.K. Guo, R.G. Cai, Y.Z. Zhang, JCAP **0505** 002 (2005);
 M.S. Berger, H. Shojaei, Phys. Rev. D **73** 083528 (2006);
 R. Rosenfeld, Phys. Rev. D **75** 083509 (2007);
 L. Amendola, G. Camargo Campos, R. Rosenfeld, Phys. Rev. D **75** 083506 (2007).
- [13] L. Parker, A. Raval, Phys. Rev. D **60** 123502 (1999);
 L. Parker, W. Komp, D. A. T. Vanzella, Astrophysical Journal, **588** 663 (2003);
 L. Parker, D. A. T. Vanzella, Phys. Rev. D **69** 104009 (2004).
- [14] L. Parker, Y. Zhang, Phys. Rev. D **44** 2421 (1991);
 Y. Zhang, Commun. Theor. Phys. **30** 603 (1998);
 Y. Zhang, Chin. Phys. Lett. **15** 622 (1998);
 Y. Zhang, Chin. Phys. Lett. **17** 76 (2000);
 Y. Zhang, Chin. Phys. Lett. **19** 1569 (2002).
- [15] Y. Zhang, Gen. Relativ. Gravit. **34** 2155 (2002);
 Y. Zhang, Gen. Relativ. Gravit. **35** 689 (2003);
 Y. Zhang, Chin. Phys. Lett. **20** 1899 (2003);
 Y. Zhang, Chin. Phys. Lett. **21** 1183 (2004).
- [16] Y. Zhang, T.X. Xia, W. Zhao, Class. Quant. Grav. **24** 3309 (2007).
- [17] W. Zhao, Y. Zhang, Class. Quantum Grav. **23** 3405 (2006);
 W. Zhao, Y. Zhang, Phys. Lett. B **690** 64 (2006);
 W. Zhao, Int. J. Mod. Phys. D **16** 1735 (2007).
- [18] T.Y. Xia, Y. Zhang, Phys. Lett. B **656** 19 (2007).

- [19] S. Wang and Y. Zhang, arXiv:0803.2760.
- [20] P. Astier, et al., *Astron. Astrophys.* **447** 31 (2006);
A.G. Riess, et al., *Astrophys. J* **656** 10 (2007).
- [21] U. Alam, V. Sahni, A.A. Starobinsky, *JCAP* **0702** 011 (2007).
- [22] V. Sahni, T.D. Saini, A.A. Starobinsky, U. Alam, *JETP Lett.* **77** 201 (2003).
- [23] J. Albert et al., [SNAP Collaboration], arXiv:astro-ph/0507458;
J. Albert et al., [SNAP Collaboration], arXiv:astro-ph/0507459;
- [24] U. Alam, V. Sahni, T.D. Saini, A.A. Starobinsky, *Mon. Not. Roy. ast. Soc.* **344** 1057 (2003).
- [25] V. Gorini, A. Kamenshchik, U. Moschella, *Phys. Rev. D* **67** 063509 (2003);
W. Zimdahl, D. Pavon, *Gen. Rel. Grav.* **36** 1483 (2004);
X. Zhang, *Phys. Lett. B* **611** 1 (2005);
X. Zhang, *Int. J. Mod. Phys. D* **14** 1597 (2005);
W.X. Wu, H.W. Yu, *Int. J. Mod. Phys. D* **14** 1873 (2005);
Z.L. Yi, T.J. Zhang, *Phys. Rev. D* **75** 083515 (2007);
B.R. Chang, H.Y. Liu, L.x. Xu, C.W. Zhang, Y.L. Ping, *JCAP* **0701** 016 (2007)
M.R. Setare, J.F. Zhang, X. Zhang, *JCAP* **0703** 007 (2007);
Y. Shao, Y.X. Gui, arXiv:gr-qc/0703111;
D.J. Liu, W.Z. Liu, arXiv:0711.4854 [astro-ph];
G. Panotopoulos, arXiv:0712.1177 [gr-qc].
- [26] W. Hao and R.G. Cai, *Phys. Lett. B* **655** 1 (2007).
- [27] J.F. Zhang, X. Zhang, H. Liu, *Phys. Lett. B* **659** 26 (2008).
- [28] W. Zhao, arXiv: 0711.2319 [gr-qc].
- [29] H. Bondi, T. Gold, *Mon. Not. R. Astron. Soc.* **108** 252 (1948).
F. Hoyle, *Mon. Not. R. Astron. Soc.* **108** 372 (1948);
F. Hoyle, J.V. Narlikar, *Proc. R. Soc. A* **270** 334 (1962);
J.V. Narlikar, *Nature*, **242** 135 (1973).